Mapping the Wildland-Urban Interface in California: A Novel Approach based on Linear Intersections

Mukesh Kumar[*1] | Vu Dao[1] | Phu Nguyen[1] | Tirtha Banerjee[1]

[1]Department of Civil and Environmental Engineering, University of California, Irvine, CA 92697, USA

[*]Corresponding author: Mukesh Kumar (mukeshk@uci.edu)

Abstract

The severity and frequency of wildfires have risen dramatically in recent years, drawing attention to the term 'wildland-urban interface' (WUI), the region where man-made constructions meet flammable vegetation. Herein, we mapped a finer-scale, novel linear WUI for California (CA) based on the intersection of boundaries of wildland vegetation and building footprint. The direct intersection is referred to as a direct WUI, whereas the intersection at 100-m is known as an indirect WUI. More fires were ignited closer to direct WUI than indirect WUI due to their proximity to communities. However, the overlap of past fire perimeters with indirect WUI is greater than that with direct WUI which shows that more areas were burned in the indirect WUI due to embers transported by strong wind gusts during large wildfires. The study's findings will help land managers and policymakers in controlling fire dangers, land-use planning, and reducing threats to fire-prone communities.

Keywords: building footprint; linear WUI; land-use planning; wildfires; wildland-urban interface; wildland vegetation

Plain Language Summary

Wildfires have become more severe and frequent in recent years, posing a threat to lives, property, and the environment. Over the years, the term 'wildland-urban interface' (WUI) has gained huge popularity in the context of wildfires. It is defined as a region where man-made structures are present within or near flammable vegetation. For more accurate analysis of wildfire occurrences and land-use planning, different WUI mapping methodologies have been developed in the past, across many countries. However, the existing approaches lack consistency in providing accurate information on the proximity of infrastructure and relief features to large flammable vegetated areas, and particularly, a clear definition of the interface. Therefore, herein, we have proposed and mapped a novel WUI, based on the linear intersection of the boundaries of flammable vegetation and individual buildings. We have thus obtained a higher-resolution WUI map that can be easily stored and accessed. Our analysis reveals that there is a higher risk of fire

ignition where vegetation is in immediate physical contact with housing communities. Results from this study will help land managers and policymakers in land-use planning, fuel management, and reducing threats to fire-prone communities.

1. Introduction

The human propensity to live within the vicinity of natural amenities offered by forested lands and seashores has been recognized in past studies (Radeloff et al., 2001; Johnson et al., 2005; Bartlett et al., 2000). Therefore, due to the increasing number of houses near forests and densely vegetated lands in the past few decades, there has been a dramatic proliferation in the number of regions where man-made structures are present within or near wildland vegetation, known as the Wildland-Urban Interface (WUI) (Radeloff et al., 2018; Martunizzi et al., 2015). In recent years, CA wildfires have burned the highest number of acres and buildings of all states in the US (National Interagency Fire Center (NIFC) report (2018); CALFIRE summary report). The wildfire season gained the title of 'giga fire' in the year 2020 and burned more than a million acres of land compared to previous years during which the burned area had been recorded as a few hundred thousand acres ('mega fire'). Whenever homes are constructed near flammable vegetation, it poses two types of major issues: first, the risk of human sparked fires increases, and second, it also escalates the risk of damage caused by wildfires (Radeloff et al., 2018).

For the purpose of a more accurate analysis of the wildfire occurrences, tracking the location of wildfires, and land use planning, different WUI mapping methodologies have been developed in the past using a wide range of datasets and for different types of man-made structural regions across many countries including Europe, Australia, and Canada (Johnston et al., 2018; Hanberry et al., 2020; Miranda et al., 2020; Bento-Gonçalves et al., 2020). In addition, these maps also depend on the context and purpose of the study; for example, housing-centric or fuel-centric WUI mapping, as demonstrated in Stewart et al., 2009. In the US, WUI mapping was based on the 2001 federal register definition of the US Department of Interior (US DOI) and the US Department of Agriculture (USDA) which states that WUI are those areas where houses are present within or nearby wildland vegetation. In the original definition, it was not specified whether the intersection of these two types of land use were based on the intersected area or the common boundary of two polygons. However, previous studies were based on areal intersection, i.e., in terms of intersection of the area of these two features and were based on zonal approaches where either a housing density was defined or point based approaches where individual housing locations were used (Radeloff et al., 2005; Wilmer and Aplet, 2005; Li et al., 2021). These approaches lacked consistency on accurate information on all three components of the WUI definition together - accurate housing

information, accurate vegetation information and a clear definition of the interface and the proximity of buildings to large vegetated areas.

To address this gap, Pereira et al., 2018 argued that a semantically correct definition of an interface (Webster's Third New International Dictionary (Gove, 1961)) should be a plane or other surface forming a common boundary of two bodies or spaces. Therefore, ideally, the result of WUI mapping would be a line segment that could show the common boundary or the physical contact between the boundaries of two features. Linear WUI offers greater simplicity in the storage and utilization of information over previous WUI mappings because each WUI line segment can be tagged with information about its surroundings, such as distance to nearby roads, fuel types, population, building and vegetation density, etc. (Pereira et al., 2018). The new WUI map for CA will yield a more accurate analysis of the wildfire events with respect to WUI as it maps at a 30-m finer-scale resolution. Recent studies suggest that most of the CA wildfires destroyed houses in the WUI but occurred outside the existing WUI regions (Kumar et al., 2020; Kramer et al., 2018). It is therefore important to analyze how far the linear WUI features are present from the past wildfire events and would be helpful in monitoring fires in proximity to these linear WUIs, as well as in making development plans in the immediate area. The distance between previous wildfire ignition points and WUI line will show how far wildfires occurred from the linear WUI. This would help in the identification of the wildfire risk prone areas. It is expected that more ignitions near the linear WUI segments due to human ignited fires. In addition, the wildfire burned area with respect to the WUI line segment will provide more information on the severity of the fire as well as the respective risk level.

The resulting linear WUI features from this approach will be in vector format as opposed to rasters, which have been provided by the previous WUI mapping approaches. In geospatial analysis, vector data are associated with higher geographic accuracy because of lesser dependence on grid size. Additionally, storing, handling, and appending new data layers to vector data is significantly more efficient compared to rasters which are considerably larger in size. In addition, vector data are much more scalable, amenable to defining connections between topology and network structures, and easier for delineating boundaries and administrative maps in fine resolution, comparable to raster datasets. Moreover, storing of vector data is possible without the loss of generalization and preserving geolocation information. Therefore, it is envisioned that developing wildland fire policies under a changing climate and growing trends in WUI land use features will be more efficient using linear WUI features as developed in this manuscript.

This paper contributes in a number of ways to existing WUI literature. To the authors' knowledge, this paper is one of the first attempts to map the linear WUI for the US using a point-based approach, i.e., the location of individual buildings at a finer resolution of 30 m and linear features. This means that rather

than providing the areas that WUIs contain, the focus of this mapping approach is the boundaries that mark the edges of the interface, which is semantically more accurate. This novel WUI map gives the most accurate representation of the intersecting boundaries between the flammable vegetation and houses. This map will guide local and regional government agencies to determine the location of infrastructures for further construction and development of buildings, roads, and power supplies, etc. Furthermore, it would also help in locating the highly risky areas where there are many communities living nearby these WUI lines and thus policies and activities will be implemented in a way to either reduce the density of houses or clear the fuel loading in such regions. The key objectives of this study are as follows: (i) map the linear WUI in terms of direct and indirect interfaces and determine which WUI is more widespread in CA; (ii) evaluate how much percentage of wildfires occurred in the linear WUI features in CA; (iii) examine the distance between wildfire ignition points and the linear WUI features to see how far the fires ignited from it since 2010 in CA. Thus, this paper aims to show the importance of the novel linear WUI features for CA at both the local and federal level.

2. Data and Methodology

2.1. Data

The vegetation data used for this study was Landsat-based, the 2016 National Land Cover Database (NLCD) (Jin et al., 2019), a new generation of NLCD products, released by the U.S. Geological Survey (USGS). We used a rasterized format of Microsoft building footprint datasets, available at 30 m spatial resolution, and used the boundaries of houses for producing the linear WUI feature (Heris et al., 2020; Li et al., 2021). Since the liner WUI was mapped using the recent land cover and housing information, therefore, to better analyze the WUI maps and their relationship with the previous wildfires, we used Monitoring Trends in Burn Severity (MTBS) datasets and included only those fires which occurred in the last decade i.e., from 2010 to 2018. It shows all 380 fire perimeters of all fire events that happened in California from 2010 to 2018 and are represented by the legend in Figure 2. More details about these data can be found in the supplementary information.

2.2. Methodology

NLCD data was clipped for California from the conterminous United States (CONUS). Clipped land cover data was converted to polygons from the original raster data using the conversion tool from the ArcGIS geoprocessing. A wildland vegetation layer was generated for WUI mapping using selection by attributes from the attribute table using ArcGIS. Only shrub/grassland, herbaceous, woody wetlands,

emergent herbaceous wetlands, and forests including evergreen, mixed, and deciduous were selected for the wildland vegetation layer (Radeloff et al., 2005; Martunizzi et al., 2015). The building raster layers were converted into vectors. The boundaries of the building were intersected with the wildland vegetated areas to map the wildland-urban interface. The resulting feature is a line, called direct WUI or indirect WUI at a 100-m buffer distance from the building boundary.

Direct WUI was calculated using the intersection tool from ArcMap using the vegetation polygon and housing boundary, and it represents the direct physical contact of buildings with the flammable vegetation. There is always a higher risk of damage to the communities living at the direct WUI feature as compared to those living at the indirect WUI as studied by Pereira et al., 2018. To map the indirect WUI, first, we took a buffer distance of 100-m from the vegetation polygon and then extracted those areas in California which had neither buildings nor vegetation using the erase tool from ArcMap. We then intersected the extracted layer with the buffered vegetation layer. Finally, we intersected the previously intersected layer with the housing boundary to get the Indirect WUI. We did not intersect the vegetation layer with a buffer and housing boundary to avoid the duplication of indirect WUI lines with the direct WUI.

3. Results and Discussions

3.1. Linear WUI features in California

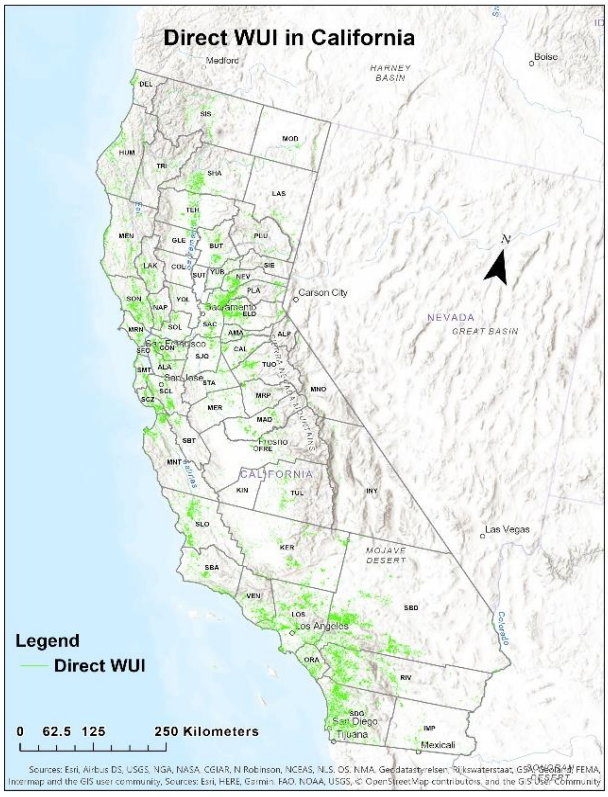

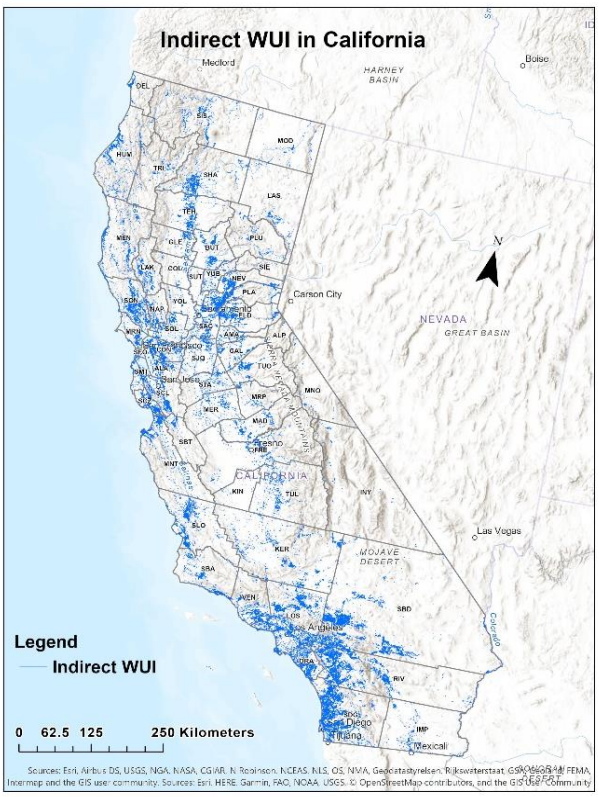

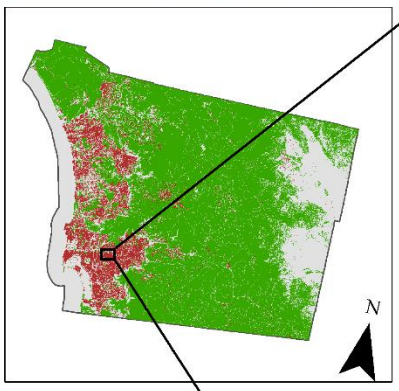

Legend

- Indirect WUI
- Direct WUI
- Non WUI
- Building Footprint
- Wildland Vegetation

0 0.25 0.5 1 Kilometers

Figure 1. The top left and top right panels show direct and indirect WUI respectively for the entire state of California. The bottom left panel on the figure above shows the spatial pattern of Microsoft building footprints and vegetation data in San Diego. A section of the County map has been enlarged to depict the direct, indirect, and non-WUI lines as well as their actual visualization at 30 m resolution. This is displayed in the bottom right panel of the figure above.

Direct WUI is a linear WUI feature that is shown in Figure 1, with pixel lengths in meters (m) and is represented with a green colorbar. Enlarged portion of Figure 1 on the bottom right panel depicts a very clear visualization of the different linear WUI (direct and indirect WUI) and Non-WUI segments and it became possible only due to the finer-scale mapping using building footprint data at 30-m resolution. In addition, such a finer-scale WUI map provides more detailed information related to both housing and wildland vegetation. Linear WUI segments may be used to gather information about building density, population and the area of the housing cluster. Similarly, it can also be used to collect data related to flammable vegetation, such as, area of the flammable patch, types of near fuel availability, and proximity to roads, etc. The findings of this analysis will help foresters, land managers, and policymakers plan future development activities, mitigation, and evacuation. Most importantly, by shrinking the linear WUI, the risk of community damage can be reduced. It can be achieved by either clearing off flammable vegetation nearby buildings or slowing down the rate at which new houses are being built near flammable vegetation.

3.2. Overlap of wildfires and linear WUI

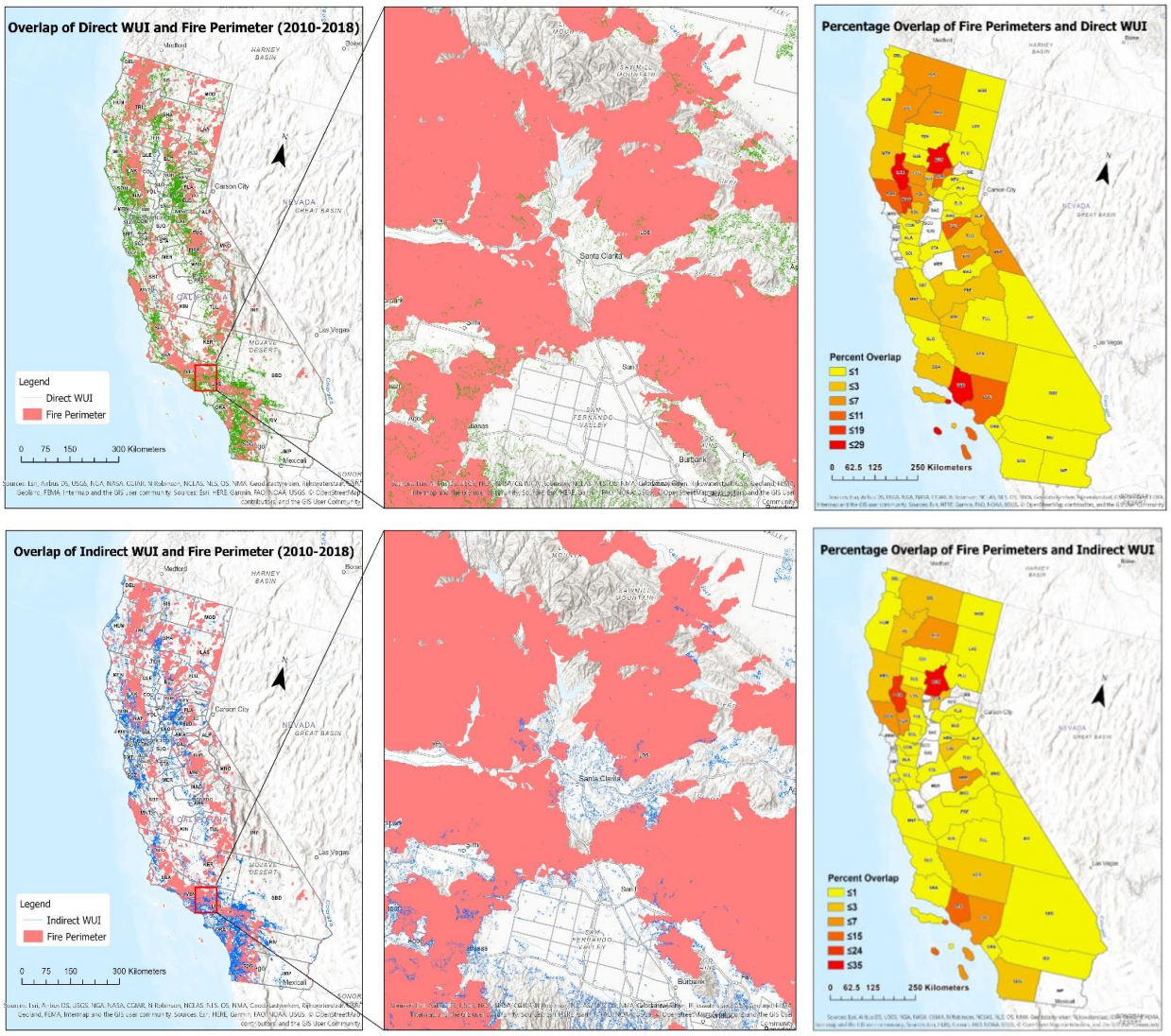

Figure 2. The figure shows the overlap of California historic wildfire perimeters (2010-2018) with direct WUI (top left panel) and indirect WUI (bottom left panel). Legends with green and blue lines represent direct and indirect WUI respectively. The middle panels present enlarged views of the relevant sections of the left two maps for clearer visualization. Top right and bottom right panel show the countywide percentage overlap of total direct WUI and total indirect WUI of California respectively with wildfire perimeters from 2010 to 2018. Colorbar shows the increase from yellow (low) to red (high) for the respective counties in California.

Right and left-hand panels in Figure 2 depict the overlap of wildfire perimeters with direct WUI from 2010 to 2018. This result clearly indicates that there is a very low percentage of overlap between the direct

WUI and the fire perimeters. However, a maximum of up to 29 % of all direct WUI lines in California overlap within the past wildfire perimeters (top right panel, Figure 2). Thus, the results show that the majority of wildfires are not occurring at WUI lines and may be burning farther away from the direct WUI lines. Similarly, a considerable percentage of fires ignited and burned outside WUI areas, according to a recent study by Kumar et al., 2020. In the case of indirect WUI, though, the percentage overlap between indirect WUI and wildfire perimeters is still low, but it is higher than what we have seen with direct WUI (top right and bottom right panels, Figure 2). Because of the devastating wildfire in Butte County in 2018, i.e., the Camp Fire, the maximum value of percentage overlap rises up to 35%. The percentage overlap of wildfire perimeters and indirect WUI might vary depending on how we choose the wildland vegetation perimeters when mapping the indirect WUI.

We calculated that the total pixel length of direct WUI in California is 119,640,741 m. It has 672,435 counts with a maximum count length of 5,958 m. In contrast, indirect WUI has a total pixel length of 164,706,030 m, which comprises a total number of 3,009,978 counts, with the highest length of a count being 5,022 m. When we examined these two linear WUI features, we discovered that the direct WUI has a lower total pixel length than the indirect WUI. However, a higher percentage of fires ignited in close proximity to direct WUI as compared to those in the vicinity of indirect WUI (Please refer to Table S1 in the supplementary materials). As a result, even though direct WUI has a lower total pixel length in California, it has a larger potential of fire ignitions in its vicinity based on prior fire incidence data. In addition, the maximum length of a count, the statistical parameters like mean, median, and mode are higher for the direct WUI. However, the total number of counts is lower for direct WUI as compared to indirect WUI. As a result, this difference in counts reveals that the direct WUI is less fragmented than the indirect WUI (Figure 1 and Figure 2). A greater length of linear WUI in a region corresponds to a higher likelihood of wildfire risk due to the presence of flammable vegetation nearby. Moreover, a greater length of linear WUI also indicates a larger number of interfaces between flammable vegetation and human settlements which would mean a higher risk of damage to the lives, properties, and health of a larger number of communities nearby that region. As mentioned earlier, the direct WUI indicates direct physical contact between houses and flammable vegetation. Hence, the likelihood of fire ignition increases as one gets closer to these linear WUI features. Interestingly, from 2010 to 2018, 36.58 % of wildfires in California were ignited within 1 km of direct WUI, according to our assessment. In the case of indirect WUI, it represents an indirect contact between the housing boundary and flammable vegetation, with a 100-meter buffer surrounding it (Pereira et al., 2018). As a result, we analyzed those house boundaries that do not cross directly with flammable vegetation, and we expected that there would be a lower likelihood of wildland fires in the presence of

such linear WUI characteristics as compared to direct WUI. Indeed, we revealed in our analysis that only 17.37 % of fires ignited within 1 km of indirect WUI. As a result, we can see that there are lower risks of wildfire ignitions closer to indirect WUI than to direct WUI.

3.3. Distance of fire ignition points from linear WUI features

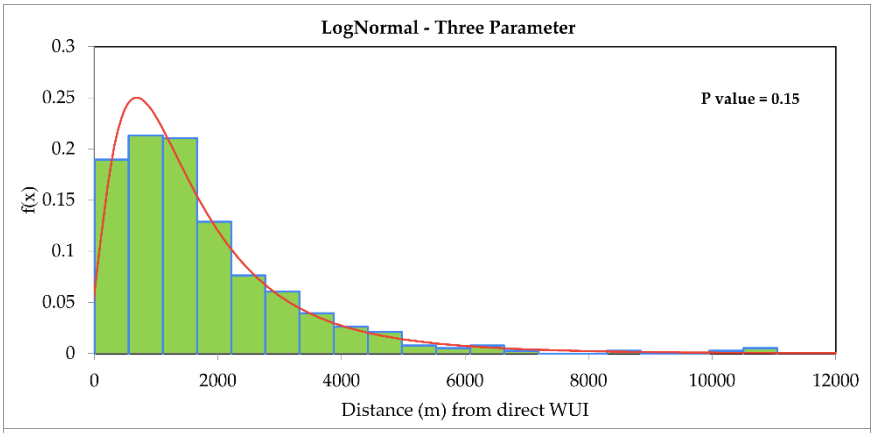

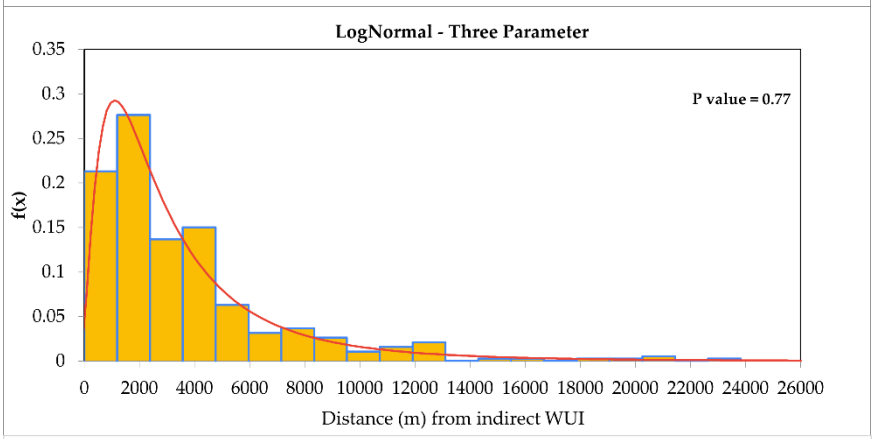

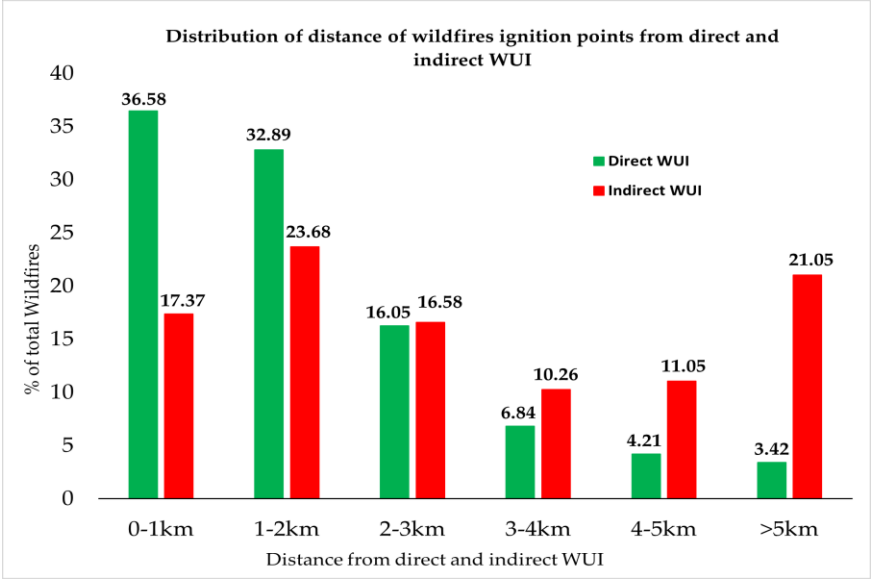

Figure 3. The figure shows the distribution of the best fit plot for distance (m) of wildfire ignition points from direct WUI (top panel) and indirect WUI (middle panel). Bottom panel shows two histograms for the distribution of distance of wildfire ignition points on the either side from linear WUI features. Histogram for the direct WUI (green) shows a continuous decreasing percentage of wildfires; while it is neither continuously increasing nor continuously decreasing and has two peaks for the indirect WUI (red).

In the bottom panel of Figure 3, we show the histogram plots for the distribution of distance of wildfire ignition points in six different classes from the direct, and indirect WUI respectively. Additionally, the percentages, total number of fires that occurred between these classes are also shown. In our analysis, we observe that in case of the direct WUI, 139 fires ignited out of a total of 380 fires i.e., 36.58% of fires ignited within 1 km range on either side from direct WUI (Please also refer to Table S1 in supplementary materials). It has decreased continuously as we increase the distance farther away from the direct WUI. And it dropped to only 3.42 % of total fires that were ignited above 5 km distance from the direct WUI in California (bottom panel, Figure 3). In case of indirect WUI, we found a different trend of the fire ignitions in different classes of the distance ranges on either side of the indirect WUI. Only 90 fires ignited within 1 km distance on either side of the indirect WUI, making it 17.37% fires within this range (Please also refer to Table S1 in supplementary materials). However, it has increased from 17.37% to 23.68% in the range of 0-1 km to 1-2 km distance from indirect WUI features respectively (bottom panel, Figure 3). Additionally, a significant portion of the fires i.e., 21.05% ignited above 5 km on either side from the indirect WUI. And this accounts for 80 fires out of a total 380 fires that ignited above 5 km in California from 2010 to 2018. We can indeed conclude that the direct WUI is more prone to fire activity based on the past nine years of wildfire history in California. And, thus, there is a higher risk of damage due to wildland fires within the closer proximity of direct WUI. On the other hand, almost 83% of fires ignited above 1 km distance from the indirect WUI. Therefore, there is lower probability of burning within 1 km distance from the indirect WUI as compared to the direct WUI. Additionally, a significant percentage of fires ignited above 5 km distance from the indirect WUI as compared to the direct WUI.

A total of 380 wildfires occurred in California from 2010 to 2018 as reported by MTBS. These included both man-made fires as well as fires ignited by natural causes, such as lightning. In the left panel of Figure S1 (Please refer to the supplementary materials), we show the countywide fire frequency in California, with more than 20 large fires in some of the counties, as shown with the red colorbar. We observe that northernmost and southern California have the highest number of fires (Figure S1, left panel). Notably in southern California, the counties of San Diego (SDG) and Kern (KER) each had 27 fires from 2010 to 2018.

While in the northern part, Siskiyou (SIS) County had a maximum of 24 fires during the same period (Please refer to Figure S1 in the supplementary materials). Strong wind events, more specifically, Diablo winds in northern California and Santa Ana winds in southern California are the main drivers for the larger and more devastating wildfires. Furthermore, human ignition is one of the most significant factors in the last few decades for a majority of the deadliest fires. Counties with zero wildfires were shown with no color and thus left blank white spaces, as can be referred to in the left panel of Figure S1. A few counties had no or very few wildfire events during 2010-2018; however, these counties more recently recorded severe wildfires that are not shown here. For example, the Silverado fire occurred in October and November 2020 in southern Orange County, California. However, such wildfire occurrences are not included in this study because of the unavailability of adequate datasets for the recent wildfire events.

It is crucial to observe how far fires ignited from the linear WUI features and which statistical curve will best fit the distribution of the distance between fires and WUI. Therefore, we performed the statistical analysis and used different curve fittings to choose the best fit curve for both direct and indirect WUI. We chose 13 different distributions to test the best fit as shown in Table S2a and Table S2b in the supplementary information. Our analysis reveals that the 'lognormal with three parameters' distribution is the best fit curve for the direct WUI as can be seen in the top panel of Figure 3. It has a p-value of 0.15 that is highest of all, as compared to the p values of the other 12 distributions (Please refer to Table S2 a and Table S2b in supplementary materials). In this approach the null hypothesis is that the dataset is sampled from the chosen distribution and a p-value larger than the significance level 0.05 indicates that the null hypothesis cannot be rejected in favor of the alternate hypothesis. Apart from p-value, there are other parameters to check whether or not the result of a statistical analysis is adequate. For example, the location and scale of a distribution also tells us about the data structure. The scale parameter describes how spread out the data values are, while the location parameter describes how large the data values are. However, some of the distributions like 'weibull' and 'gamma' do not have these parameters (Please refer to Table S2 a and Table S2b in supplementary materials). And therefore, we must check for the 'shape' parameter, which is an outcome of these distributions. The shape parameter describes how the data is spread. In general, a larger scale results in a more spread-out distribution. In this study, we used a suitable number of datasets (380) to perform the statistical analysis in both direct and indirect WUI (Please refer to Table S2 a and Table S2b in supplementary materials). Therefore, the conclusion of our results based on p value is adequate and acceptable. As we can see in the middle panel of Figure 3, lognormal with three parameters is also the best fit curve in the case of indirect WUI.

4. Conclusions

Past studies showed that different WUI maps were developed for the CONUS using a variety of datasets and different mapping methodologies. However, neither of these focused on WUI mapping based on the linear intersection of vegetation and housing boundary, using building footprint and NLCD land cover data respectively. In this study, we mapped linear WUI at 30 m resolution. We defined two types of linear WUI i.e., direct, and indirect WUI for California. Direct WUI has direct physical contact between flammable vegetation and housing boundary and thus, has a higher risk of fires. While indirect WUI is mapped by the intersection of housing, and 100 m buffer boundary surrounding flammable vegetation and therefore it has a lower probability of fires. Results revealed that the direct WUI had a lower total pixel length and is less scattered than the indirect WUI in California. However, a higher percentage of fires ignited in the vicinity of direct WUI because of a higher extent of human activities as compared to indirect WUI. Hence, even though direct WUI has a lower total pixel length in California, it has a larger potential of fire ignitions in its vicinity based on the historical wildfires. Furthermore, the majority of wildfires did not burn along WUI lines, and we found that the overlap between wildfire burned areas and WUI hardly goes up to 30% for some of the counties. The reason for this is simply because some of the recent fires occurred over these linear WUIs. Furthermore, the percentages are lower in most of the counties in California as wildfires did not burn directly over it, but in the vicinity of linear WUI features. As revealed in this study, 69.47% fires ignited within 2 km range from direct WUI and 41.05% ignited within the same range from indirect WUI in California. Therefore, in this study, we show that the direct WUI are more prone to wildfires as compared to the indirect WUI. Not only this but also, the fires ignited from the linear WUI features follow a 'lognormal with three parameters' distribution in both direct and indirect WUI. Results from this study show that most of the wildfire events in CA have occurred within 2 km linear distance from these linear WUI features and this study also proposes that fires are not happening at the intersecting lines, but they ignite farther away from the linear WUI features as highlighted in Kumar et al., 2020. These linear WUI maps will help in creating and sustaining a fire-adapted community within a WUI. This would also help policymakers to develop a community wildfire protection plan in the era of climate change that will bring an increase in wildfire events in the future. In addition, it will enhance community awareness regarding the prevention of fires within the WUI. Overall, this research will help in creating a more effective response to the wildfire events that will occur in the WUI.

Acknowledgments

M. Kumar and T. Banerjee acknowledge the funding support from the University of California Laboratory Fees Research Program funded by the UC Office of the President (UCOP), grant ID LFR-20-653572. Additional support was provided by the new faculty start up grant provided by the Department of Civil and Environmental Engineering, and the Henry Samueli School of Engineering, University of California, Irvine.

Data and material availability

All data used and generated in this study is limited to private use only. However, it will be made available for public use after publication.

Author Contributions

Mukesh Kumar: Conceptualization, Methodology, Software, Data curation, Writing- Original draft preparation, Visualization, Investigation, Software, Validation, Writing-Reviewing and Editing; **Vu Dao:** Investigation, Visualization; **Phu Nguyen:** Methodology, Software; **Tirtha Banerjee:** Conceptualization, Supervision, Reviewing and Editing, Project administration, Funding acquisition.

Conflicts of Interest

The authors declare no conflict of interest.

References

Bartlett, J.G., Mageean, D.M. and O'Connor, R.J., 2000. Residential expansion as a continental threat to US coastal ecosystems. *Population and Environment*, *21*(5), pp.429-468.

Bento-Gonçalves, A. and Vieira, A., 2020. Wildfires in the wildland-urban interface: Key concepts and evaluation methodologies. *Science of the total environment*, *707*, p.135592.

Bond, W. Fires, Ecological Effects of. In Encyclopedia of Biodiversity, Volume 2; Academic Press: Cambridge, MA, USA, 2001; pp. 745–753.

Demuzere, M., Hankey, S., Mills, G., Zhang, W., Lu, T. and Bechtel, B., 2020. Combining expert and crowd-sourced training data to map urban form and functions for the continental US. *Scientific data*, *7*(1), pp.1-13.

Glickman, D. and Babbitt, B., 2001. Urban wildland interface communities within the vicinity of federal lands that are at high risk from wildfire. *Federal Register*, *66*(3), pp.751-777.

Gove, P. B. (1961). Webster's Third New International Dictionary of the English Language, unabridged. (P. B. Gove, Ed.). Springfield, Mass.: G&C Merriam Company.

Hanberry, B.B., 2020. Reclassifying the Wildland–Urban Interface Using Fire Occurrences for the United States. *Land*, *9*(7), p.225.

Headwater Economics, November 2020: https://headwaterseconomics.org/natural hazards/structures-destroyed-by-wildfire/

Heris, M.P., Foks, N.L., Bagstad, K.J., Troy, A. and Ancona, Z.H., 2020. A rasterized building footprint dataset for the United States. *Scientific Data*, *7*(1), pp.1-10.

Homer, C., Dewitz, J., Jin, S., Xian, G., Costello, C., Danielson, P., Gass, L., Funk, M., Wickham, J., Stehman, S. and Auch, R., 2020. Conterminous United States land cover change patterns 2001–2016 from the 2016 national land cover database. *ISPRS Journal of Photogrammetry and Remote Sensing*, *162*, pp.184-199.

Jin, S., Homer, C., Yang, L., Danielson, P., Dewitz, J., Li, C., Zhu, Z., Xian, G. and Howard, D., 2019. Overall methodology design for the United States national land cover database 2016 products. *Remote Sensing*, *11*(24), p.2971.

Johnson, K.M., Nucci, A. and Long, L., 2005. Population trends in metropolitan and nonmetropolitan America: Selective deconcentration and the rural rebound. *Population Research and Policy Review*, *24*(5), pp.527-542.

Johnston, L.M. and Flannigan, M.D., 2018. Mapping Canadian wildland fire interface areas. *International journal of wildland fire*, *27*(1), pp.1-14.

Jolly, W.M., Cochrane, M.A., Freeborn, P.H., Holden, Z.A., Brown, T.J., Williamson, G.J. and Bowman, D.M., 2015. Climate-induced variations in global wildfire danger from 1979 to 2013. *Nature communications*, *6*(1), pp.1-11.

Kramer, H.A., Mockrin, M.H., Alexandre, P.M., Stewart, S.I. and Radeloff, V.C., 2018. Where wildfires destroy buildings in the US relative to the wildland–urban interface and national fire outreach programs. *International Journal of Wildland Fire*, *27*(5), pp.329-341.

Kramer, H.A., Mockrin, M.H., Alexandre, P.M. and Radeloff, V.C., 2019. High wildfire damage in interface communities in California. *International journal of wildland fire*, *28*(9), pp.641-650.

Li, S., Dao, V., Kumar, M., Nguyen, P. and Banerjee, T., 2021. Mapping the wildland-urban interface in CA using remote sensing data. ESSOAR Preprints, doi: 10.1002/essoar.10507343.3

Martinuzzi, S., Stewart, S.I., Helmers, D.P., Mockrin, M.H., Hammer, R.B. and Radeloff, V.C., 2015. The 2010 wildland-urban interface of the conterminous United States. *Research Map NRS-8. Newtown Square, PA: US Department of Agriculture, Forest Service, Northern Research Station. 124 p.[includes pull-out map].*, *8*, pp.1-124.

Miranda, A., Carrasco, J., González, M., Pais, C., Lara, A., Altamirano, A., Weintraub, A. and Syphard, A.D., 2020. Evidence-based mapping of the wildland-urban interface to better identify human communities threatened by wildfires. *Environmental Research Letters*, *15*(9), p.094069.

Monitoring Trends in Burn Severity (2019) Monitoring Trends in Burn Severity (MTBS). Available at http://www.mtbs.gov/.

M. Kumar, S. Li, P. Nguyen, T. Banerjee, ESSOAr (2020). Revisiting the existing definitions of wildland-urban interface for California. doi/10.1002/essoar.10504449.1

National Interagency Fire Center (NIFC), 2018 and 2019 report.

Pereira, J., Alexandre, P., Campagnolo, L., Bar Massada, A., Radeloff, V. and Silva, P., (2018). Defining and mapping the wildland-urban interface in Portugal. VD Xavier: Advances in Forest Fire Research, pp.743-749

Radeloff, V.C., Hammer, R.B., Voss, P.R., Hagen, A.E., Field, D.R. and Mladenoff, D.J., 2001. Human demographic trends and landscape level forest management in the northwest Wisconsin Pine Barrens. *Forest Science*, *47*(2), pp.229-241.

Radeloff, V.C., Hammer, R.B., Stewart, S.I., Fried, J.S., Holcomb, S.S. and McKeefry, J.F., 2005. The wildland–urban interface in the United States. *Ecological applications*, *15*(3), pp.799-805

Radeloff, V.C., Helmers, D.P., Kramer, H.A., Mockrin, M.H., Alexandre, P.M., Bar-Massada, A., Butsic, V., Hawbaker, T.J., Martinuzzi, S., Syphard, A.D. and Stewart, S.I., 2018. Rapid growth of the US wildland-urban interface raises wildfire risk. *Proceedings of the National Academy of Sciences*, *115*(13), pp.3314-3319.

Stewart, S.I., Wilmer, B., Hammer, R.B., Aplet, G.H., Hawbaker, T.J., Miller, C. and Radeloff, V.C., 2009. Wildland-urban interface maps vary with purpose and context. *Journal of Forestry*, *107*(2), pp.78-83.

Stewart, S.I., Radeloff, V.C., Hammer, R.B. and Hawbaker, T.J., 2007. Defining the wildland–urban interface. *Journal of Forestry*, *105*(4), pp.201-207.

Wildfire Today, 2020. Available at https://wildfiretoday.com/2020/09/21/community-destruction-during-extreme-wildfires-is-a-home-ignition-problem/

Wilmer, B. and Aplet, G., 2005. Targeting the community fire planning zone: Mapping matters. *The Wilderness Society: Washington, DC, USA*.

Mapping the Wildland-Urban Interface in California: A Novel Approach based on Linear Intersections

Mukesh Kumar*[1] | Vu Dao[1] | Phu Nguyen[1] | Tirtha Banerjee[1]

[1]Department of Civil and Environmental Engineering, University of California, Irvine, CA 92697, USA

*Corresponding author: Mukesh Kumar (mukeshk@uci.edu)

Supplementary Information

Table S1. Statistical summary table showing distance of fire ignition points with respect to direct and indirect WUI in California.

Distance from Indirect WUI (km)	No. of wildfires (2010-2018)		Percentage of total fires (%)	
	Indirect	Direct	Indirect	Direct
0-1	66	139	17.37	36.58
1-2	90	125	23.68	32.89
2-3	63	62	16.58	16.05
3-4	39	26	10.26	6.84
4-5	42	16	11.05	4.21
>5	80	13	21.05	3.42

Table S2a. Statistical analysis using 13 different curve fittings to choose the best fit curve for the distribution of the distance between wildfire ignition points and direct WUI line segments.

Descriptive Statistics and curve fitting summary table for direct WUI									
	Count	*Mean*	*StDev*	*Median*	*Min*	*Max*	*Skew*	*Kurt*	
	380	1741.6	1554.6	1425.9	4.689	11056	2.388	9.107	
Distribution	**Location**	**Shape**	**Scale**	**Threshold**	**Log-Likelihood**	**AD**	**p Value**	**LRT**	**AIC**
Gamma		1.358	1282.5		-3205.7	0.699	0.084		6415.5
Weibull		1.190	1849.9		-3206.7	0.871	0.026		6417.4
Gamma - Three Parameter		1.374	1269.9	-3.155	-3205.7	0.652	0.105	0.777	6417.4
Weibull - Three Parameter		1.184	1844.0	2.734	-3206.6	0.896	0.023	0.662	6419.2
LogNormal - Three Parameter	7.383		0.700	-300.7	-3209.0	0.553	0.153	0.000	6424.1
LogLogistic - Three Parameter	7.319		0.438	-197.2	-3213.6	0.982	0.006	0.000	6433.1
Exponential - Two Parameter			1736.9	4.689	-3214.8	5.856	<0.001	0.152	6433.5
Exponential			1741.6		-3215.8	5.736	<0.001		6433.6
LogLogistic	7.148		0.556		-3221.9	2.637	<0.005		6447.8
Largest Extreme Value	1124.8		965.5		-3234.4	2.620	<0.01		6472.7
LogNormal	7.051		1.058		-3239.9	5.891	0.000		6483.8
Normal	1741.6		1552.5		-3331.3	15.07	0.000		6666.6
Smallest Extreme Value	2656.4		2542.8		-3496.3	44.68	<0.01		6996.6

Table S2b. Statistical analysis using 13 different curve fittings to choose the best fit curve for the distribution of the distance between wildfire ignition points and indirect WUI line segments.

Descriptive Statistics and curve fitting summary table for indirect WUI									
	Count	*Mean*	*StDev*	*Median*	*Min*	*Max*	*Skew*	*Kurt*	
	380	3599.8	3535.2	2492.7	2.939	23825	2.339	7.327	
Distribution	**Location**	**Shape**	**Scale**	**Threshold**	**Log-Likelihood**	**AD**	**p Value**	**LRT**	**AIC**
LogNormal - Three Parameter	7.921		0.836	-265.6	-3481.1	0.243	0.766	0.000	6968.2
Gamma		1.278	2816.1		-3485.1	1.294	<0.005		6974.1
Gamma - Three Parameter		1.286	2801.4	-2.505	-3485.0	1.304	<0.005	0.773	6976.0
Weibull		1.119	3762.2		-3487.6	1.830	<0.01		6979.3
LogLogistic	7.803		0.564		-3487.8	0.740	0.032		6979.5
Weibull - Three Parameter		1.117	3758.5	1.337	-3487.6	1.825	<0.01	0.820	6981.2
Exponential			3599.8		-3491.7	3.784	<0.001		6985.4
Exponential - Two Parameter			3596.9	2.939	-3491.4	4.013	<0.001	0.431	6986.7
LogLogistic - Three Parameter	7.800		0.578	2.936	-3493.0	0.820	0.019	*	6991.9
LogNormal	7.749		1.046		-3500.8	1.982	0.000		7005.6
Largest Extreme Value	2232.3		2047.1		-3531.0	6.813	<0.01		7066.1
Normal	3599.8		3530.6		-3643.5	22.39	0.000		7291.0
Smallest Extreme Value	5674.7		5511.1		-3796.6	46.64	<0.01		7597.2

1. Data in detail

1.1. Vegetation data

The vegetation data used for this study was Landsat-based, the 2016 National Land Cover Database (NLCD) (Jin et al., 2019), a new generation of NLCD products, released by the U.S. Geological Survey (USGS). It was designed specifically for the rapidly growing demand for land cover change analysis and the related studies, and it represented the most robust land cover base ever produced by the USGS. It included land cover and its changes over the CONUS for seven years, 2001, 2003, 2006, 2008, 2011, 2013, and 2016. Thus, it increased the land cover time series from 10 years to 15 years (2001 to 2016) (Homer et al., 2020). It was downloaded from Multi-Resolution Land Characteristics (MRLC) Consortium (available on https://www.mrlc.gov/) and was available at 30 m spatial resolution. The accuracy and robustness of the NLCD 2016 map were also shown by recent studies including Jin et al., 2019 and Homer et al., 2020. NLCD 2016 could be used for the identification of the different features at a finer resolution and thus can be considered for the deeper analysis of the expanding areas and further planning of the developmental activities. It contained a total of 28 different types of land cover classes over the CONUS. For the purpose of mapping the linear WUI, we chose only those vegetation categories which were flammable vegetation (right panel, Figure S1) and included shrubland, grassland, woody wetlands, and all kinds of forest vegetation (California fire alliance 2001; Radeloff et al., 2005). Specific steps used for extracting the vegetation layer using ArcMap tools will be discussed in methodology section 2.2.

1.2. Building data

With the improvement of remote sensing data in acquisition efficiency and resolution, it has become possible to extract detailed housing boundaries from it. Over the past few years, Microsoft has made great efforts in applying deep learning, computer vision, and Artificial Intelligence for mapping, and leveraging the power of Machine Learning in analyzing satellite imagery to trace the shape of buildings across the country. More specifically, Bing Maps, a mapping platform from Microsoft had successfully generated the first comprehensive high-quality housing footprints database covering the entire CONUS by using Deep Neural Network (DNN) and the residual neural network (ResNet34) with segmentation techniques (Refine Net up-sampling) to detect individual building footprints from their imagery data. However, there was a need to develop some methodologies to put this data in a more usable format for the researchers and land planning management, to study and analyze the human and environmental impacts on small cities and regions (Heris et al., 2020; Demuzere et al., 2020). A new method of rasterizing building footprint was developed by Heris et al., 2020 and was used in this study to produce a robust WUI map. Taking advantage

of the new building dataset from Microsoft product and rasterizing method, we propose a new framework of mapping novel linear WUI over California. The building dataset was extracted from the Microsoft dataset containing 124,885,597 computer-generated building footprints in GeoJSON format for the US. Regarding the accuracy metrics, the precision of the evaluation set is 99.3 % and the recall is 93.5 %. The California building footprint file implemented in this study contained 10,988,525 computer-generated building footprints in California and was extracted from the US building footprint dataset by Microsoft (2018), then converted to shapefile format. We used a rasterized format of Microsoft building footprint datasets, available at 30 m spatial resolution, and used the boundaries of houses for producing the linear WUI feature (Heris et al., 2020; Li et al., 2021). This boundary data was obtained from Heris et al., 2020 in which the value of each cell represents the area of the cell that was covered by building footprints. The cell values were calculated by developing an algorithm that used High Performance Computing (HPC) (Heris et al., 2020). This algorithm created a small meshgrid (a 2D array) for each building's bounding box, generating unique values for each meshgrid cell that was further coordinated with NLCD products to make it more usable (projected using Albers Equal Area Conic system) (Heris et al., 2020). The range of values was from 0 to 900 sq. meters. To better aid the implementation of building footprint data into large-scale computation, these values are represented as raster layers with a 30 m cell size covering each of the 48 conterminous states.

1.3. Wildfires data

Previous wildfire data were downloaded from Monitoring Trends in Burn Severity (MTBS), (available on https://www.mtbs.gov/direct-download). MTBS is an interagency initiative whose purpose is to continuously monitor the intensity of wildfires in terms of burn severity and the size of major fires from 1984 to present in the US. It does not cover small fires and includes all those fires in the Western US of 1000 or more acres, and 500 or greater acres in the Eastern part of the US (MTBS, 2021). In this study, we used two kinds of MTBS datasets, namely, wildfire occurrence dataset that showed wildfire ignition points, and burned area boundaries datasets, representing wildfire perimeters. For analyzing the overlap of previous wildfires with the linear WUI features, we used wildfire perimeter. While detecting the distance of previous wildfire events from the linear WUI features, we used wildfire ignition points data. Since the liner WUI was mapped using the recent land cover and housing information, therefore, to better analyze the WUI maps and their relationship with the previous wildfires, we included only those fires which occurred in

the last decade i.e., from 2010 to 2018. It shows all 380 fire perimeters of all fire events that happened in California from 2010 to 2018 and are represented by the legend in Figure 2.

2. Wildland fire ignition frequency analysis

A total of 380 wildfires occurred in California from 2010 to 2018 as reported by MTBS. These included both man-made fires as well as fires ignited by natural causes, such as lightning. In the left panel of Figure S1, we show the countywide fire frequency in California, with more than 20 large fires in some of the counties, as shown with the red colorbar. We observe that northernmost and southern California have the highest number of fires (left panel, Figure S1). Notably in southern California, the counties of San Diego (SDG) and Kern (KER) each had 27 fires from 2010 to 2018. While in the northern part, Siskiyou (SIS) County had a maximum of 24 fires during the same period. Strong wind events, more specifically, Diablo winds in northern California and Santa Ana winds in southern California are the main drivers for the larger and more devastating wildfires. Furthermore, human ignition is one of the most significant factors in the last few decades for a majority of the deadliest fires. Counties with zero wildfires were shown with no color and thus left blank white spaces, as can be referred to in the left panel of Figure S1. A few counties had no or very few wildfire events during 2010-2018; however, these counties more recently recorded severe wildfires that are not shown here. For example, the Silverado fire occurred in October and November 2020 in southern Orange County, California. However, such wildfire occurrences are not included in this study because of the unavailability of adequate datasets for the recent wildfire events.

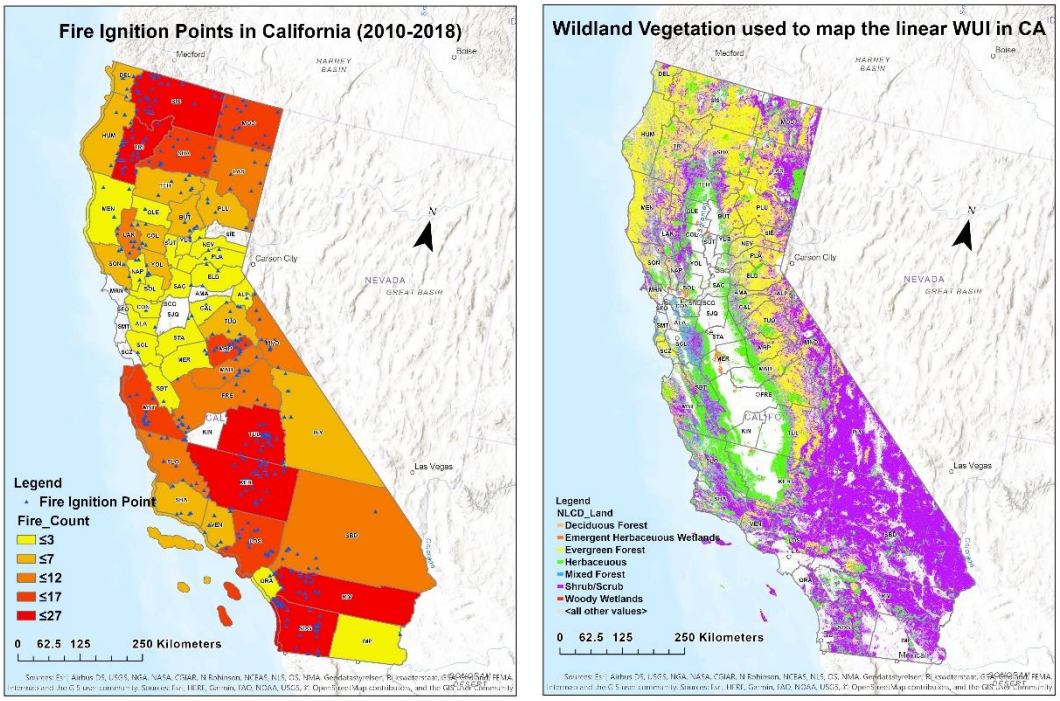

Figure S1. The left panel on the figure above shows wildfire frequency in all the counties of California from 2010 to 2018. The blue triangular-shaped symbols represent the wildfire ignition points in the respective counties, while the colorbar shows the number strength of these fire frequencies for each County. The white portions of the map represent those counties where the fire activity was absent. The right panel on the figure above shows the spatial pattern of NLCD data, the wildland vegetation data used to map the linear WUI for California at 30 m resolution; it includes three kinds of forest, shrubs, and emergent herbaceous & woody wetlands; white color represents the water bodies and other vegetation types that were not included for mapping the linear WUI.

Figure S1 (right panel) depicts the wildland vegetation cover used in the mapping of linear WUI. This map clearly shows that the majority of southern California is covered by shrubland vegetation, whereas the dominant land cover type in the north is evergreen forest and shrubland. Furthermore, the variability in land cover type is greater in the northern counties of California than in the southern regions. Overall, shrubland is the most common type of vegetation in California. Shrublands are defined as ecosystems with a minimum of 30% shrub or sub-shrub cover and tree densities of up to 10 trees per hectare (USDA). They are one of the significant regions where wildfire season lasts the longest (Jolly et al., 2015). Although it has a low fuel presence, those available fuels are very dry and therefore, the fire spread is very high in shrublands (Bond et al., 2001). Also, recent studies have shown that the shrublands are one of the areas

most affected by wildfires (Jolly et al., 2015). The white colorbar in the right panel of Figure S1 also reflects water and other land cover types that are not classified as wildland vegetation while mapping linear WUI.